Cent. Eur. J. Geosci. • 2(2) • 2010 • 175-187
DOI: 10.2478/v10085-010-0007-6

VERSITA

Central European Journal of **Geosciences**

Calcium-aluminum-silicate-hydrate "cement" phases and rare Ca-zeolite association at Colle Fabbri, Central Italy

Research Article

F. Stoppa[1]*, F. Scordari[2], E. Mesto[2], V.V. Sharygin[3], G. Bortolozzi[4]

1 *Dipartimento di Scienze della Terra, Università G. d'Annunzio, Chieti, Italy*

2 *Dipartimento Geomineralogico, Università di Bari, Bari, Italy*

3 *Sobolev V.S. Institute of Geology and Mineralogy, Siberian Branch of the Russian Academy of Sciences, Novosibirsk 630090, Russia*

4 *Via Dogali, 20, 31100-Treviso*

Received 26 January 2010; accepted 8 April 2010

Abstract: Very high temperature, Ca-rich alkaline magma intruded an argillite formation at Colle Fabbri, Central Italy, producing cordierite-tridymite metamorphism in the country rocks. An intense Ba-rich sulphate-carbonate-alkaline hydrothermal plume produced a zone of mineralization several meters thick around the igneous body. Reaction of hydrothermal fluids with country rocks formed calcium-silicate-hydrate (CSH), i.e., tobermorite-afwillite-jennite; calcium-aluminum-silicate-hydrate (CASH) – "cement" phases – i.e., thaumasite, strätlingite and an ettringite-like phase and several different species of zeolites: chabazite-Ca, willhendersonite, gismondine, three phases bearing Ca with the same or perhaps lower symmetry of phillipsite-Ca, levyne-Ca and the Ca-rich analogue of merlinoite. In addition, apophyllite-(KF) and/or apophyllite-(KOH), Ca-Ba-carbonates, portlandite and sulphates were present. A new polymorph from the pyrrhotite group, containing three layers of sphalerite-type structure in the unit cell, is reported for the first time. Such a complex association is unique. Most of these minerals are specifically related to hydration processes of: (1) pyrometamorphic metacarbonate/metapelitic rocks (natural analogues of cement clinkers); (2) mineralization between intrusive stocks and slates; and (3) high-calcium, alkaline igneous rocks such as melilitites and foidites as well as carbonatites. The Colle Fabbri outcrop offers an opportunity to study *in situ* complex crystalline overgrowth and specific crystal chemistry in mineral phases formed in igneous to hydrothermal conditions.

Keywords: hydrothermal• melilitolite • high temperature metamorphism • Italian alkaline magmatism

1. Introduction

The Colle Fabbri (CF) outcrop was described initially by Stoppa [1] and consists of a kalsilite-leucite-wollastonite-

*E-mail: fstoppa@unich.it

melilitolite plug associated with extrusive breccias. We refer the reader to Stoppa and Rosatelli [2] and Stoppa and Sharygin [3] for detailed descriptions of the volcanology and petrology at CF. Leucite melilitolites are relatively common in Italy compared to other areas of alkaline magmatism [4]. Other examples of wollastonite melilitolite are from Mt. Vulture [5], a mafic alkaline volcano located in the Lucania Region of Italy, which displays a wide range of mafic to alkaline, Ca-rich volcanic rocks, with melilitolite, ijolite, soevite, Ne-syenite ejecta together with mantle xenoliths [6].

The CF mineral association was sampled at the inner part of a large thermal aureole (Figure 1). Our interest in the mineralization stems from its rarity and unusual chemistry, reflecting conditions related to chemical exchange between the melt, the argillite country rock and the hydrothermal system. The assemblage includes minerals that roughly span the range of the Ca:Si ratios seen in wollastonite $Ca_3[Si_3O_9]$ and rankinite $Ca_3[Si_2O_7]$, and are typical of hydration products. These phases are interesting because of their variety of crystal structure, the peculiarity of the transformation processes in which they are involved, and their chemical variations. They are predominantly calcium-silicate-hydrate (CSH), calcium-aluminum-silicate-hydrate (CASH), silicate-sulphate-carbonates (SSC) and aluminum-phosphate-sulphate (APS). CSH and CASH are "cement" phases that can be artificially obtained by the reaction of portlandite $Ca(OH)_2$ and silica gel in the presence of sulphate-alkaline water fluids [7–9]. In nature, these minerals occur in metacarbonate xenoliths in silicate lavas, as well as contact mineralization [10–14], and in larnitic rocks of the Hatrurim pyrometamorphic formation, Israel [15, 16]. Carbonatites and high-calcium igneous rocks, such as melilitite/melilitolite and ijolite, also contain CSH minerals [17]. Ettringite has been recently reported from Vulture carbonatite [6].

Wheeler et al. [18], who first reported the occurrence of Willhendersonite at CF, stressed the importance of a number of rare zeolites at this locality. Zeolites often form together with CSH and CASH, but in this case define a very specific association with kamafugitic (kalsilite, melilite/foidite) outcrops occurring in Italy, Germany and a few other localities throughout the world [19]. This peculiar association of CSH-CSAH with rare zeolites with high Ca and high-alkaline igneous rocks represents a convergence of very specific geological conditions.

The aims of this paper are: 1) to describe the mineralization developed in a rare and unusual geologic context; 2) to understand the mineralogical sequences; and 3) to point out possible new phases originating from igneous to hydrothermal conditions during chemical exchange between melts and argillitic country rocks.

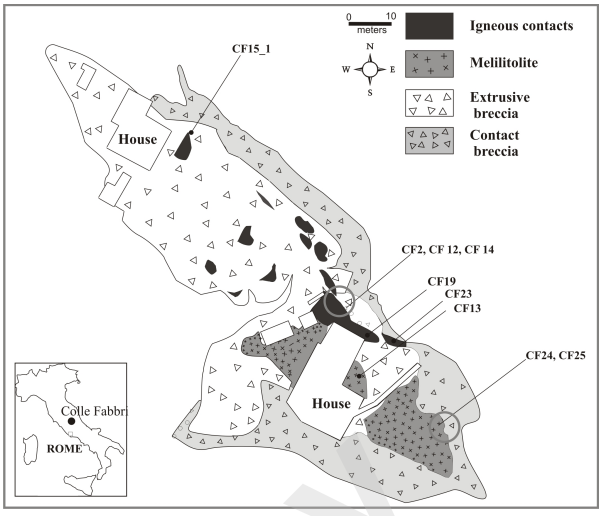

Figure 1. Sampling sites at the Colle Fabbri igneous outcrop.

2. Methods

All of the secondary minerals identified at CF so far were carefully selected using a binocular microscope, prior to scanning electron microscopy (SEM) work using both secondary electron (SE) and back scattered electron (BSE) images. SEM microprobe analyses in EDS mode were carried out using a JEOL 6380LA scanning electron microscope at the V.S. Sobolev Institute of Geology and Mineralogy (IGM), Novosibirsk, Russia. The operating conditions were as follows: accelerating voltage of 20-25 kV, a probe current of 1 nA, and a pressure of 20-60 Pa. Further identification was achieved using morphology, electron microprobe analysis (EMPA) in WDS mode, X-ray powder diffraction profiles, and lattice parameter refinements. Electron microprobe analyses (EMPA) were made at IGM, Novosibirsk, using a "CAMEBAX-micro" electron microprobe. The operating conditions for all minerals were as follows: beam diameter of 1-2 μm, an accelerating voltage of 20 kV, a beam current of 15-20 nA, and a counting time of 10 s for all elements. Data reduction was performed using a PAP routine. Precision for major and minor elements was better than 2 and 5%, respectively. Standards used for quantification of the major elements in Fe-rich sulphide were: troilite (Fe-Kα, S-Kα), chalcopyrite (Cu-Kα) and Fe-Ni-Co alloy (Ni-Kα, Co-Kα). Overlap corrections for Fe-Kβ - Co-Kα were made. The following standards were used for quantification of the major and minor elements in silicates and other phases:

Table 1. Formula unit, cell parameter and space group of minerals identified at Colle Fabbri. Locations of the rock samples from which the mineral sample labels are derived can be found in Figure 1.

Crystal	CF2_4(a)	CF2_4(b)	CF2_2_1	CF12_1	CF14_1
Refls. used for lattice params	906 Reflections	304 Reflections	35 Reflections	371 Reflections	247 Reflections
Crystal size [mm]	0.060×0.105×0.145	0.060×0.105×0.145	0.050×0.070×0.200	0.060×0.070×0.150	0.015×0.020×0.200
Theta max	19.15°	19.15°	11.51°	26.27°	18.47°
Crystal	CF15_1	CF16_1	CF16_2	CF17_1	CF19_1
Refls. used for lattice params	1544 Reflections	237 Reflections	290 Reflections	626 Reflections	2551 Reflections
Crystal size [mm]	0.050×0.070×0.200	0.010×0.045×0.110	0.010×0.065×0.100	0.020×0.060×0.155	0.39×0.39×1.50
Theta max	34.72°	19.49°	20.49°	19.79°	41.60°
Crystal	CF22_2	CF23_4	CF23_5	CF24_2	CF25_1
Refls. used for lattice params	40 Reflections	1052 Reflections	1994 Reflections	647 Reflections	1338 Reflections
Crystal size [mm]	0.42×42×0.750	0.045×0.145×0.150	0.050×0.100×0.100	0.020×0.070×0.195	0.045×0.090×0.090
Theta max	11.51°	23.15°	28.67°	26.53°	28.01°

Mn-rich garnet (Fe-Kα, Mn-Kα), diopside (Ca-Kα, Mg-Kα, Si-Kα), albite (Na-Kα), ilmenite (Ti-Kα), orthoclase (K-Kα, Al-Kα), fluorapatite (P-Kα), Sr- and Ba-rich synthetic silicate glasses (Sr-Lα, Ba-Lα), anhydrite (S-Kα), chlorapatite (Cl- Kα). Overlap corrections were performed for the following elements: Ti-Kα - Ba-Lα; Si-Kα - Sr-Lα.

Single crystal X-ray diffraction (SCXRD) analysis was sometimes necessary in order to identify ambiguous species. Identification was made at the Dipartimento Geomineralogico at Bari University using a Bruker-X8 diffractometer equipped with a four-circle Kappa goniometer and a 4K APEX-II CCD detector. Experimental parameters are summarised in Table 1. All data were collected at ambient temperature using a combination of $\phi\omega$ scans and MoKα radition ($\lambda\alpha$ 0.71073 Å). Exposure time per frame was chosen as a function of the scattering power of the studied crystal, and varied from 10 to 120 s per frame. Cell refinement, absorption correction, and study of the intensity statistic were performed with the SAINT [20], SADABS programs [21] and XPREP [22] software. Relevant crystallographic data for SCXRD investigated crystals are summarized in Table 1.

In Table 2 we summarize the phases, formula units, cell parameters and space groups of the secondary minerals at CF, some of which were identified by chemical and XRD investigations, and some only by XRD analysis. Microprobe data for some of the relevant minerals quoted in Table 2.

3. Mineral assemblage

The samples come from the brecciated contact between the plug and the metamorphosed argillite (Figure 1). The host rock is a complex mixture of quenched, contaminated melt composed mainly of Wo-An-Cpx and glass infiltrating a vesicular clinker breccia which contains cordierite, $(Mg,Fe^{2+})_2(Al_2Si)^{[4]}[Al_2Si_4O_{18}]$ and tridymite, SiO_2. The mineral assemblages described in this paper occur in amygdales and in joints, which clearly post-date solidification of the igneous body. The amygdales contain concentric layers of fibrous or microcrystalline phases and cannot be texturally regarded as having crystallized from the melt, but are likely to have been formed by alkaline hydrothermal fluids. The igneous body has cooling joints and fractures, which are also mineralized. Much smaller amounts of secondary minerals are found in the igneous rock matrix as substitution reaction/alteration products. Some of the CF phases are likely to be gels, which have more variable composition and poorer definition than the equivalent crystalline phases.

Table 2. Formula unit, cell parameter and space group of minerals identified at Colle Fabbri.

Sample	Crystal	Mineral	Unit Formula	Cell Parameters (Å)				Space group
				a	b	c	β	
CF2	CF2_4 (a)	Overgrowth of Chabazite-Ca and Levyne-Ca	$(Ca_{2.410}\ Sr_{0.096}\ Ba_{0.016}\ Na_{0.003}\ K_{0.015}\ Mn_{0.006}\ Fe^{2+}_{0.003}s)_{\Sigma 2.55}\ [(Al_{4.991}\ Si_{6.987})\ O_{24}]$ $11.15H_2O\ \Sigma^+=48.00\ \Sigma^-=48.00$	13.801(3)	-	15.020(3)	90	$R\bar{3}$
	CF2_4 (b)		$(Ca_{1.749}\ Na_{0.018}\ Ba_{0.001}\ K_{0.759})_{\Sigma 2.53}\ [(Al_{4.323}\ Si_{13.688})\ O_{36}]\ 12.43H_2O\ \Sigma^+=72.00$ $\Sigma^-=72.00$	13.41(1)	-	23.06(2)	90	$R\bar{3}$
	CF2_2_1	Levyne-Ca	$(Ca_{3.336}\ Sr_{0.082}\ Ba_{0.002}\ Na_{0.019}\ K_{0.122}\ Fe^{2+}_{0.013}\ Mg_{0.015}\ Al_{0.072})_{\Sigma 3.66}\ [(Al_{7.251}\ Si_{10.749})\ O_{36}]$ $15.89H_2O\ \Sigma^+=72.00\ \Sigma^-=72.00$	13.44(5)	-	23.08(9)	90	$R\bar{3}$
CF12	CF12_1	Strätlingite	$(Ca_{1.790}\ Sr_{0.019}\ Fe^{2+}_{0.001}\ Mg_{0.001}\ Ba_{0.002}\ Na_{0.004}\ K_{0.009}\ Al_{0.083})_{\Sigma 1.91}\ Al\ [(Al_{0.886}\ Si_{1.114})$ $O_2\ (OH)_{10}]\ 2.76H_2O\ \Sigma^+=14.00\ \Sigma^-=14.00$	5.772(2)	-	37.945(5)	90	$R\bar{3}$
CF14	CF14_1	Thaumasite	$Ca_6\ Si_2^{[6]}\ [(OH)_{12}\ (CO_3)_2\ (SO_4)_2]\cdot 24H_2O$ Identified solely by SCXRD	11.066(5)	-	10.459(3)	90	$P6_3$
CF15	CF15_1	Vertumnite[a]	$(Ca_{1.902}\ Sr_{0.022}\ Ba_{0.048}\ Na_{0.010}\ K_{0.009}\ Al_{0.027}\ Fe^{2+}_{0.002}\ Mg_{0.002})_{\Sigma 2.02}\ Al\ [(Al_{1.057}\ Si_{1.193})$ $O_3\ (OH)_9]\ 3.38H_2O\ \Sigma^+=15.00\ \Sigma^-=15.00$	5.7403(4)	5.7406(4)	25.143(4)	119.96(1)	$P2_1$
CF16	CF16_1	Apophyllite-(KOH)	$KCa_4[(OH,F)Si_4O_{10}]\cdot 8H_2O$ Identified solely by SCXRD	9.038(2)	-	15.950(6)	90	$P4/mnc$
	CF16_2	X1	$(Ca_{5.741}\ Ba_{0.003}\ Mg_{0.004}\ Mn_{0.001}\ Na_{0.016}\ Al_{0.142}\ K_{0.004}\ Fe^{2+}_{0.001})_{\Sigma 5.91}\ (Al_{1.952}\ Si_{0.048})$ $[(SO_4)_{3.001}\ (OH)_{12}]3.30H_2O\ \Sigma^+=36.00\ \Sigma^-=36.00$	11.237(4)	-	21.468(7)	90	$P31c$
CF17	CF17_1	Apophyllite-(KOH)	$KCa_4\ [(OH,F)\ Si_4O_{10}]\cdot 8H_2O$ Identified solely by SCXRD	9.0185(8)	-	15.873(2)	90	$P4/mnc$
CF19	CF19_1	Pyrrhotite	$Fe_{(1-x)}S$ Identified solely by SCXRD	6.9261(7)	-	17.220(1)	90	$R\bar{3}$
CF22	CF22_2	Apophyllite-(KF)	$(K_{0.977}\ Na_{0.025})_{\Sigma 1.00}\ (Ca_{3.923}\ Mg_{0.007}\ Al_{0.056})_{\Sigma 3.99}\ Si_{7.991}\ O_{20}\ (F,OH)11.45H_2O$ $\Sigma^+=41.00\ \Sigma^-=41.00$	8.98(1)	-	15.77(2)	90	$P4/mnc$
CF23	CF23_4	X2	$(Ca_{4.026}\ Ba_{0.217}\ K_{0.667}Na_{0.090}\ )_{\Sigma 5.00}\ (K_{2.007}\ Mg_{0.032}\ Fe^{2+}_{0.014}\ Mn_{0.004})_{\Sigma 2.06}\ [(Al_{11.099}$ $Si_{20.838})\ O_{64}]\ 18.41H_2O\ \Sigma^+=128.00\ \Sigma^-=128.00$	14.368(3)	14.394(4)	9.954(2)	90	$P2_12_12_1$
	CF23_5	X3	$(Ca_{2.098}\ Ba_{0.095}\ Na_{0.013}\ K_{0.612}\ Fe^{2+}_{0.017}\ Al_{0.162})_{\Sigma 3.00}\ [(Al_{5.530}\ Si_{10.470})\ O_{32}]\ 12.99H_2O$ $\Sigma^+=64.00\ \Sigma^-=64.000$	9.828(1)	14.359(1)	8.759(1)	124.16(1)	$P2_1$
CF24	CF24_2	Phillipsite-Ca	$(Ca_{2.514}\ Ba_{0.004}\ Na_{0.104}\ K_{1.213}\ Mg_{0.003}\ Fe^{2+}_{0.009})_{\Sigma 3.85}\ [(Al_{6.347}\ Si_{9.645})\ O_{32}]\ 11.70H_2O$ $\Sigma^+=64.00\ \Sigma^-=64.00$	10.030(1)	14.362(1)	8.777(1)	124.98(1)	$P2_1/m$
CF25	CF25_1	X4	$(Ca_{2.542}\ Ba_{0.010}\ Na_{0.115}\ K_{1.053}\ Mg_{0.003}\ Mn_{0.002}\ Fe^{2+}_{0.002})_{\Sigma 3.73}\ [(Al_{6.300}\ Si_{9.704})\ O_{32}]\ 10.012(1)$ $9.87H_2O\ \Sigma^+=64.00\ \Sigma^-=64.00$		14.362(1)	8.789(1)	124.74(1)	$P2_1$

[a]Pseudohexagonal structure. Unique axis *c*

4. Identification and description of mineral phases

4.1. CSH

Tobermorite, $Ca_5Si_6O_{16}(OH)_2 \cdot 7H_2O$ [23] occurs in white mammillary aggregates up to 500 μm across that have a vitreous lustre. High magnification SEM images show that aggregates are composed of several individual crystals of about 5–20 μm in diameter (Figure 2B). Tobermorite occurs at CF in two varieties: a 14 Å-tobermorite and an 11 Å-tobermorite, with compositions that differ in their water content and periodicities along the silicate chains. For more details see [24].

Jennite, $Ca_9Si_6O_{18}(OH)_6 \cdot 8H_2O$, appears in acicular crystals up to 0.5 mm along the *b* axis, usually grouped together to form tight bundles or radial aggregates. It has a whitish colour and vitreous lustre. It often occurs in the innermost part of concentrically layered amygdales, which contain a core of amorphous silica, microcrystalline calcite, aragonite and ettringite (Figure 3F). Very recent structural studies have clarified the structural arrangements of both jennite and an alteration product of jennite with lower H_2O content [23, 24]. Jennite is a rare mineral usually found in association with thaumasite in vugs of the famous Kalyango carbonatite lava at Fort Portal, Uganda [17].

Afwillite, $Ca_3[SiO_3OH]_2 \cdot 2H_2O$, forms rare transparent columnar prisms, which are elongated and striated and usually associated with jennite (see above) or apophyllite, $(Na, K)Ca_4[(OH,F) \cdot (Si_4O_{10})_2] \cdot 8H_2O$, thaumasite and ettringite (see below). Interestingly the type locality is the Dutoitspan and Wessels diamond mines, Kimberley, South Africa [25].

4.2. CASH

The intensity statistics have been used here to obtain indicative information about the centre of symmetry, although structural refinement may change this and is planned for the near future. Ettringite, thaumasite, strätlingite and vertumnite can all derive from chemical decomposition of CSH by sulphate solutions.

Ettringite, $Ca_6Al_2[(SO_4)_3(OH)_{12}] \cdot 26H_2O$, occurs in small globular aggregates that have a pale yellowish colour and a matt lustre. The globules form the innermost part of concentrically layered amygdales that have internal vugs. Substitution of Al for Si and partial replacement of $(SO_4)^{2-}$ with $(CO_3)^{2-}$ may lead to the formation of solid solution between ettringite and thaumasite minerals but, considering the dissimilar structure, it is more likely to show the intergrowths of the two minerals. Ettringite evolves to thaumasite or poorly crystalline material when in contact with $CaCO_3$ and silica gel. In contrast with thaumasite, ettringite is very clearly identified under a scanning microscope and microprobe because of transformation into metaettringite during the preparation of samples for analysis (carbon coating and vacuumization). This is due to dehydroxylation under the condition $T > 50°C$ [26].

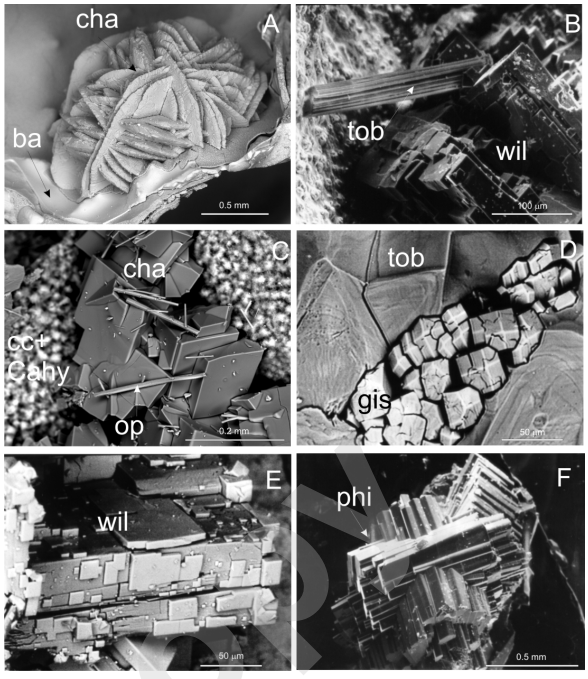

Figure 2. Zeolites. A. Chabazite-Ca; B. Willhendersonite with associated tobermorite. The field of view is mainly occupied by tabular crystals of willhendersonite intimately associated with chabazite showing typical [0001]-twins (SEM-BSE image); C. chabazite-Ca with opal pseudomorphs, calcite and Ca-hydrosilicate aggregates; D. Gismondine crystals (0.5–1 mm) on tobermorite (SEM-BSE image). Electron bombardment damage has produced the cracked appearance of the pseudo-octahedral crystals; E. Willhendersonite crystals in "trellis-like" twinning (SEM-BSE image); F. Phillipsite crystals (0.5–1 mm): fourlings or twins of higher rank (SEM-SE image). Mineral symbols Cha= chabazite, ba= barite, tob= tobermorite, wil= willhendersonite, op= opal, gis= gismondine phi= phillipsite.

Thaumasite, $Ca_6Si_2[(CO_3)_2(SO_4)_2(OH)_{12}] \cdot 24H_20$, is ubiquitous in the CF rocks, occurring in felt-like aggregates of limpid, colourless-to-whitish crystals. Parallel, elongated hexagonal prisms up to 1 mm along the *c* axis are common. It is a late mineral, forming after microcrystalline calcite, tobermorite and amorphous silica. Microcrystalline aggregates of gypsum, $Ca[SO_4] \cdot 2H_2O$ and calcite are found as an alteration product after thaumasite. These associations tend to support the hypothe-

Table 3. Representative EMP analyses of Colle Fabbri secondary mineral for some relevant crystals quoted in Table 2.

Sample	CF2_1_1	CF2_4(a)	CF2_4(b)	CF12_1	CF15_1	CF16_2	CF22_2	CF23_4	CF23_5	CF24_2	CF25_1
Mineral	Chabazite-Ca		Levyne-Ca	Stratlingite	Vertunmite	X1[a]	Apophyllite	X2[a]	X3[a]	X4[a]	X5[a]
SiO_2	42.8	41.0	58.7	16.4	16.4	0.34	50.2	49.3	47.8	44.0	45.6
Al_2O_3	24.74	24.85	15.73	24.6	24.3	12.7	0.3	22.28	22.03	24.58	25.10
FeO	0.06	0.02	0.00	0.01	0.03	0.01	-	0.04	0.09	0.05	0.01
MnO	0.00	0.04	0.00	0.01	0.02	0.01	0.00	0.01	0.00	0.00	0.01
MgO	0.04	-	0.00	0.01	0.02	0.02	0.03	0.05	0.00	0.01	0.01
CaO	12.4	13.2	7.0	24.6	24.4	38.3	23.00	8.89	8.9	10.7	11.1
BaO	0.02	0.24	0.01	0.08	1.70	0.05	0.04	1.31	1.11	0.05	0.11
SrO	0.56	0.97	0.00	0.48	0.51	-	-	-	0.00	0.00	0.00
Na_2O	0.04	0.01	0.04	0.03	0.07	0.06	0.08	0.11	0.03	0.25	0.28
K_2O	0.38	0.07	2.55	0.10	0.10	0.02	4.81	4.96	2.19	4.34	3.88
SO_3	-	-	-	-	-	28.58	-	-	-	-	-
Sum	81.0	80.4	84.0	66.3	67.6	80.1	78.5	87.0	82.1	84.0	86.1

[a]See text.

sis that the formation of this mineral involves the effect of "sulphatizing" fluids on carbonate-silicate rocks in a low pressure, low temperature (<100°C) environment in a post-zeolitic stage of mineralization. This mineral has been identified by SCXRD (Table 1). There are actually three minerals that can be described by the same chemical formula: thaumasite, jouravskite and carraraite, given by $Ca_6X^{4+}_2[(OH)_{12}(CO_3)_2(SO_4)_2]\cdot 24H_2O$, where X^{4+} = Si, Mn and Ge, respectively. All three compounds have very similar lattice parameters (a = b ≈ 11, c ≈ 10.50 Å), the same crystal system (hexagonal) and with the exception of carraraite, which is centrosymmetric, the same space group $P6_3$ [27].

The intensity statistics and systematic absences show that the compound analyzed here is likely non-centrosymmetric (< E^2–1 ⩾ 0.744), with a primitive cell and a hexagonal screw axis 6_3. This result and the absence of Ge exclude the carraraite option, and agree with the qualitative chemical analyses that indicate the occurrence of Si, Al and Ca cations. The lack of the Mn^{4+} identifies the mineral as thaumasite. Finally, the presence of Al as well as the chemical variability of Si and Ca leave open interesting mineralogical questions.

Strätlingite, $Ca_2Al[(AlSi)O_2(OH)_{10}]\cdot 2.25H_2O$ and *vertumnite* $(Na,K)Ca_4[(Si_4O_{10})_2(OH,F)]\cdot 8H_2O$, form whitish hexagonal platy crystals up to 100μm across, which are intergrown and possibly twinned (Figure 3C). They were identified by the Gandolfi diffraction pattern but neither this method nor the SEM/EDS investigations allowed a clear distinction of strätlingite from its polytype, vertumnite [28]. Further investigations performed in this work by means of SCXRD technique confirmed the occurrence of both polytypes, strätlingite (CF12) and vertumnite (CF15) (see Table [2]). Intensity statistics of the CF12_1 crystal suggest the space group $R\bar{3}$ instead $R\bar{3}m$, as found by [28]. Another difference concerns a greater amount of water (2.76 vs. 2.25 H_2O per formula unit (p.f.u.)), as shown in Table 2. CF15_1 has been identified as vertumnite. The lattice parameters of the CF15_1 crystal are very similar to those quoted in the literature, but the intensity statistics suggest that the crystal is non-centrosymmetric. This symmetry, the lattice, and the systematic absences support the assignment of the $P2_1$ space group to the mineral instead of $P2_1/m$ [29]. The crystal's chemical formula shows Ca^{2+} to be the dominant extra-framework cation, as expected, even if the amount of water (3.28 H_2O p.f.u.) exceeds the 2.45 H_2O p.f.u. confirmed by [29]. The occurrence of this mineral at CF is one of only a handful found globally.

4.3. Zeolites

The list given below follows the nomenclature for zeolite minerals recommended by the IMA-CNMMN subcommittee on zeolites [30].

4.3.1. Chabazite and Levyne

Chabazite-Ca, $(Ca_{0.5}, K, Na)_4[Al_4Si_8O_{24}]\cdot 12H_2O$ (Figure 2A), was found co-existing with *levyne-Ca*, $(Ca_{0.5}, Na, K)_6[(Si_6\ Al_{12}O_{36}]\cdot \sim 17H_2O$ in the same crystal (Figure 4B). The overgrowth was confirmed by both EPMA and by SCXRD studies, with different chemical compositions and reciprocal lattice parameters *c* corresponding to more than one phase that occurred in different propor-

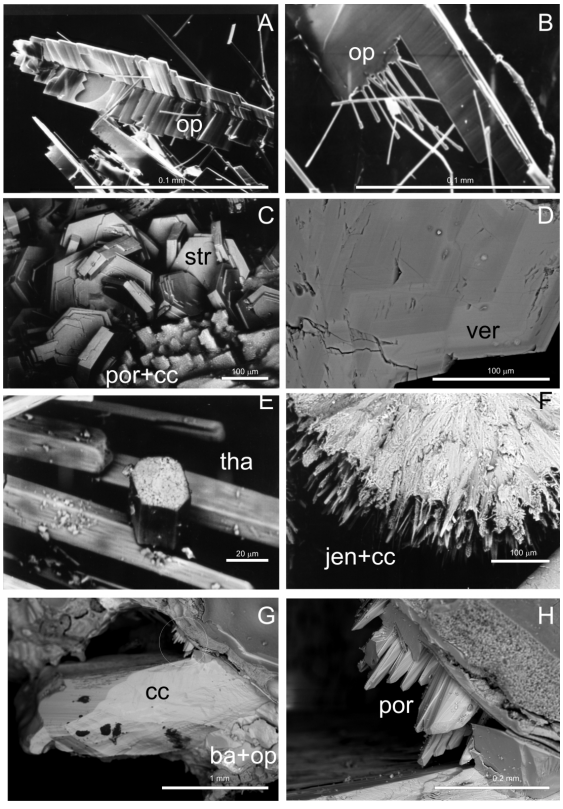

Figure 3. CSH and others. A and B. Amorphous silica pseudocrystals with platy and fibrous morphology. The largest individual mimics growth bands, such as one would expect of a "proper" crystal, although it does not yield any X-ray diffraction lines (SEM-BSE image); C. Strätlingite/vertumnite crystals with typical hexagonal morphology. The concave appearance of the tops of the crystals is responsible for the typical pearlaceous lustre of the mineral (SEM-BSE image). D. Vertumnite, BSE image, in which optical zoning is pronounced, but chemical zoning is poor and mainly produced by Ba; E. Sheaf-like crystal aggregates of thaumasite (SEM-BSE image); F Jennite in typical tufts of very thin needles on calcite (SEM-BSE image); G. calcite; H. portlandite (enlarged from the circled area in the previous photo). Mineral symbols as in Figure 2 plus str= strätlingite, por= portlandite, cc= calcite, ver= vertumnite, tha= thaumasite, jen= jennite.

tions. Chabazite-Ca and levyne-Ca (Table 2) have similar a lattice parameters (13.80 and 13.41 Å respectively) but different c constants. c values are 15.02 and 23.06 Å for chabazite-Ca and levyne-Ca, respectively. The similarity of the symmetry ($R\bar{3}$) and of the a lattice parameter explains the intergrowth of these two minerals. Crystals form colourless, transparent to milky-white, pseudocubic rhombohedra with typical [0001]-twinning, normally 300 μm in size (Figure 2C). Unlike that shown in Table 2, CF chabazite contains unusually high amounts of Ba. The walls of the cavities hosting chabazite and phillipsite are lined in places by a very thin veneer of barite, $Ba[SO_4]$. The semi-quantitative EDS analyses of chabazite showed some variation in the Si:Al ratios, the absolute predominance of Ca as an exchangeable cation with very little K substitution, and occasionally high Ba contents (up to 2.1 wt% BaO). Table 2 shows two cation partitions obtained from two distinct analysis points carried out on the same crystal by EMPA. One of them (CF2_4(a)) corresponds to chabazite-Ca, while the other one CF2_4(b) is similar to levyne-Ca.

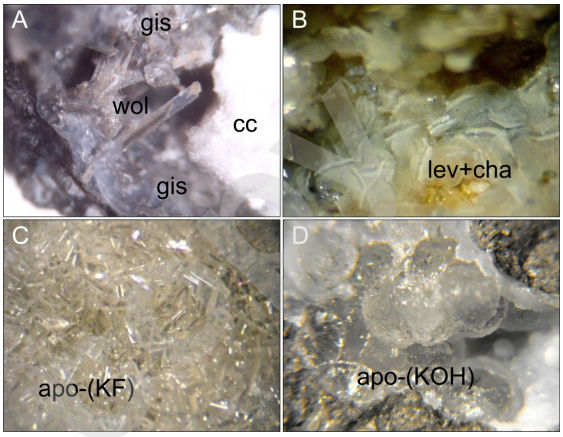

Figure 4. Micro photos. A. Gismondine and wollastonite on calcite; B. Levyne-Ca plus chabazite-Ca, C. Apophyllite-(KF);, D. Apophyllite-(KOH). Mineral symbols as in Figures 2 and 3 plus wol= wollastonite, lev= levyne, apo-(KF) = apophyllite-(KF), apo-(KOH)= apophyllite-(KOH).

X-ray diffraction analysis of the same crystal allowed measurement of 1259 ($I > 5\sigma(I)$) reflections). Of these, 906 (~ 72% of total collected reflections) could be indexed on the basis of the following cell parameters: $a = b = 13.801(4)$, $c = 15.020(3)$, $\alpha = \beta = 90°$, and $\gamma = 120°$. Of the 353 remaining reflections, 304 (~ 24% of total collected reflections) were indexed on the basis of the following constants: $a = b = 13.41(1)$, $c = 23.06(2)$, $\alpha = \beta = 90°$, and $\gamma = 120°$. The intensity statistic performed on both chabazite-Ca and levyne-Ca points to $R\bar{3}$ as the most probable symmetry instead of $R\bar{3}m$ [31]. In summary, chemical and X-ray analyses suggest that the crystal investigated is a combination of two crystals intergrown under different conditions. As shown in Table 2, in chabazite there is considerably more Ca, and considerably less K and especially Si, than in levyne. Taking into account both crystallographic and chemical data, another crystal from the same sample has been identified as levyne-Ca. A careful inspection of the crystals found in the CF2 matrix leads us to conclude that another phase, as yet unidentified, is also present. This phase seems to have much more Mg, K and Na but much less Ca and Al than levyne-Ca.

Willhendersonite, $KCa[Al_3Si_3O_{12}]\cdot 6H_2O$, forms transparent, colourless or whitish, tabular crystals of up to 200 μm that form trellis-like twin intergrowths at right angles (Figure 2B, E). A qualitative analysis carried out by SEM investigations shows that the K and Ca contents are highly variable, with Ca/K ratio always >1. Willhendersonite associated with other zeolites is even rarer, with few occurrences so far reported in the world. Included among these are: 1) the San Venanzo and Cupaello twin occurrences [32, 33], which are regionally associated with the CF, Italy; 2) Styria, Austria [34] and 3) the Eifel region, Germany [14, 19, 35].

4.4. Gismondine

Gismondine, $Ca[Al_2Si_2O_8]\cdot 4.5H_2O$, is an uncommon zeolite, rare at CF, and has only been found in the amygdales in the main igneous body. The crystals show a pseudo-octahedral habit, are transparent, colourless to greyish in colour with a vitreous lustre and reach up to 1 mm across (Figure 2D and Figure 4A).

4.5. Phillipsite

Phillipsite-Ca, $(K, Na, Ca_{0.5}, Ba_{0.5})_x [Al_xSi_{16-x}O_{32}]\cdot 12H_2O$, is abundant at CF but is confined to the amygdales. Its morphology is typically a short pseudo-orthorhombic prism with *a*-elongation and shows simple twinning or fourlings (Figure 2F). The crystals are colourless and transparent with a vitreous lustre and are usually <1 mm across. The chemical composition of phillipsite shows a variable and sometimes high Ba content. Three crystals, named CF23_5, CF24_2 and CF25_1 in Table 2, appear similar to phillipsite-Ca in chemistry, but two of these (CF23_5 and CF25_1) are different in terms of space groups ($P2_1$ instead of $P2_1/m$). To emphasize this uncertainty, these two minerals were reported as X3 and X4 (see Table 2). Examining each of the three crystals separately, we observe that the crystal system and lattice parameters of the CF23_5 sample (Table 2) resemble those of phillipsite, with substantial Ca [36–38]. According to [37], phillipsite-K was found to be monoclinic, with space group $P2_1/m$, constants $a = 9.8881(5)$, $b = 14.404(8)$ and $c = 8.6848(5)$ Å and $\beta = 124.271(3)°$. The compound analyzed here, quite different from those studied by [36–38], seems to be non-centrosymmetric ($< E^2 - 1 > = 0.812$) with space group $P2_1$.

It is useful to compare the chemical formula with those from other studies:

- $(Ca_{2.098}Ba_{0.095}Na_{0.013}K_{0.612}Fe^{2+}_{0.017}Al_{0.162})_{\Sigma 3.00}$ $[(Al_{5.532}Si_{10.470})O_{32}]12.99H_2O$ [this study],
- $K_{\sim 2}$ $Ca_{\sim 1.5}$, $Na_{\sim 0.4}$ $Al_{\sim 5}Si_{\sim 10}$ O_{32} $12H_2O$ [36],
- $K_{2.44}Ca_{1.56}Na_{0.82}[(Al_{6.4}Si_{9.6})O_{32}]$ $10.26H_2O$ [37],
- $K_{1.74}Ca_{0.70}Na_{1.58}[(Al_6Si_{16})O_{32}]$ 10.97 H_2O [38].

The comparison shows that Ca instead of K is the dominant extra-framework cation in our crystal.

The CF24_2 crystal has similar crystal system and space group to phillipsite-Ca [36], i.e. monoclinic and $P2_1/m$ ($< E^2 - 1 > = 1.042$). From a chemical point of view, the main difference is a greater amount of Ca, but lower K and extra-framework cations.

The cell parameters and symmetry of CF25_1 were found to be similar to the compound already described above (CF23_5). The intensity statistics suggest the same space group $P2_1$ with $< E^2 - 1 > = 0.789$. The main points of dissimilarity concern more Ca and K in the extra-framework sites, greater Al in tetrahedral sites, and lower water content in CF25_1. The crystal structure solution will clarify the peculiarities of all three crystals from the investigated outcrop.

4.6. Ca-K zeolite

Ca-K zeolite (CF23_4 in Table 2) is similar to merlinoite, $K_5Ca_2[Al_9Si_{23}O_{64}]\cdot 22H_2O$, quoted in the literature as being orthorhombic with lattice parameters a = 14.116(7), b = 14.229(6) and c = 9.946(6) Å and space group Immm [27]. Even if the lattice parameters are similar (see Table 2) important dissimilarities are observed between merlinoite and the compound at hand. The first is centrosymmetrical with space group Immm, while our compound seems non-centrosymmetrical ($< E^2 - 1 \geqslant 0.774$, which is close to the expected value for non-centrosymmetrical structures, i.e. 0.736) with space group $P2_12_12_1$. For this reason the label X2 has been assigned to this mineral (see Table 2). When the chemical formula quoted in Table 2 is considered and compared with the simplified one assigned to merlinoite:

- $(Ca_{4.026}Ba_{0.217}K_{0.667}Na_{0.090})_{\Sigma 5.00}$ $(K_{2.007}Mg_{0.032}Fe^{2+}_{0.014}Mn_{0.004})_{\Sigma 2.06}$ $[(Al_{11.099}Si_{20.838})$ $O_{64}]18.41H_2O$ [this study],
- K_5 Ca_2 $[Al_9$ Si_{23} $O_{64}]22H_2O$ [40].

We note that bivalent (Ca, Ba) and monovalent (K, Na) cations present in our compound substitute for the K and Ca, respectively, in merlinoite. This chemical and crystallographic data lead us to believe that this is a new mineral and therefore further investigations by SCXRD are planned for future work to determine its crystal structure.

4.6.1. Phyllosilicates

Apophyllite-(KF), $(K,Na)Ca_4Si_8O_{20}(F,OH)\cdot 8H_2O$ and *apophyllite*-(KOH) are frequently found associated with

zeolites (Figure 4C and D). At CF they occur at the contact between the melt and the clinker. They resemble zeolites and have rings, with the terminal non-bridging tetrahedral apexes of the four member rings pointing alternatively up and down along the c axis. Adjoining layers are based on these rings. Rings are opposing one another and form a Si-O-Ca-O-Si type of bond with the interim Ca-ions. This structure forms a void and, therefore, resembles a zeolite structure.

Two mineralogical species were detected in the sample labelled CF16; apophyllite and a species similar to ettringite (CF16_2). The CF16_1 crystal has been identified as apophyllite-(K,OH) based only on SCXRD analysis. No chemical analyses were carried out for this crystal.

The crystal labelled CF16_2 has been shown to be a very dehydrated ettringite, and because of this has been named X1 in Table 2. The unit cell parameters, crystal system and space group *P*31c are the same as those quoted for ettringite [41]. Moreover, like ettringite, the formula indicates that the dominant extra-framework cation is Ca. Assuming that Al and Si replace each other in the same site, the tetrahedral cations are in the ratio 2:3 = (Al,Si):S, also similar to ettringite. However we observe that the water content in our compound is markedly lower than that of ettringite (3.30 vs. $26H_2O$ p.f.u.). A compound obtained as a dehydroxylation product of ettringite, namely metaettringite, was previously studied by [26], who showed that the electron diffraction patterns of ettringite and metaettringite are similar, with the *a* parameter of the latter considerably shorter than that of the former (8.5 vs. 11.23 Å). According to [26], the structure of metaettringite could not be solved by the SCXRD technique even though two computer-based models illustrating its atomic structure were suggested by the authors. Following Zhou et al. [26], a more reliable model of dfs phases (despujolsite, fleischerite, schaurteite) with space group $P\bar{6}2c$ and $M^{2+}_6M^{4+}_2(SO_4)(OH)_{12}\cdot 6H_2O$ composition (M^{2+}= Ca, Pb and M^{4+}= Mn, Ge) is proposed. We cannot, of course, rule out other possible alternative structures.

The investigated compound reveals interesting questions on the metaettringite crystal structure. Among these are: is it possible to obtain a trustworthy model based on experimental single crystal data; what is the real water content of this phase; and is the model proposed by [26] suitable to describe a further phase? The solution of these and other questions concerning metaettringite is deferred to a later paper.

Only one mineralogical species was found in the CF17 sample, and the crystal tested by SCXRD, CF17_1, was found to be apophyllite-(KOH) or apophyllite-(KF). No chemical analysis was performed on this crystal. CF22_2 crystal, now characterized by both chemical and single crystal investigations, seems to be apophyllite-(KF), with lower lattice parameter than those shown by CF16_1 and CF17_1 analogues.

4.6.2. Sulphates and carbonates

Aragonite, $CaCO_3$, rarely found at CF, forms finely-dispersed material in the microcrystalline aggregates of calcite and ettringite associated with jennite. Identification was obtained solely by X-ray powder diffraction; no individual crystals could be detected, even with the SEM.

Calcite, $CaCO_3$, is the most abundant secondary mineral at CF. It mantles other minerals and commonly forms multiple white, microcrystalline layers associated with amorphous silica and tobermorite. Discrete, transparent crystals of up to 1.5 mm, with an elongate trapezohedral habit, occur in amygdales found in the igneous body.

Gypsum, $CaSO_4\cdot 2H_2O$, possibly an alteration product of thaumasite, was identified by X-ray diffraction methods and SEM-EDS investigation from the presence of Ca and S in the EDS spectrum.

Barite, $BaSO_4$, present in many amygdales and fractures, forms thin, small, microcrystalline veneers coating the walls of the cavities or even the other crystals within the cavities. Due to its microcrystalline occurrence, identification was based on SEM observations in the BSE mode and EDS elemental identification. Confirmation was based on X-ray powder diffraction.

4.6.3. Others minerals

Pyrrhotite (CF19_1) is a compound in an interesting phase belonging to the pyrrhotite group. A qualitative chemical analysis by SEM shows that only Fe and S are present in its structure. In addition, X-ray diffraction data seems to indicate that 3 sphalerite-type layers are in the unit cell of this phase, so potentially it can bridge the gap between troilite (pyrrhotite-2H) and pyrrhotite-4M. According to reflection statistics the symmetry seems to be rhombohedral, although only the structure solution can determine this conclusively.

Magnetite (Ti-rich), $Fe^{2+}Fe^{3+}O_4$, forms discrete octahedral crystals up to 20µm across, possibly associated with cryptocrystalline cordierite and amorphous silica.

Opaline silica, $SiO_2\cdot nH_2O$, has been deposited in almost all cavities in the CF rocks. It consists of concentrically arranged layers showing a milky, white colour and pearly lustre. It also forms lamellae and thin needles up to 3 mm long that are colourless and transparent and have a vitreous lustre (Figure 3A and B). Based on single crystal X-ray investigations, it is found to be amorphous. The morphological features probably result from pseudomorph growth after tridymite. The EDS analyses always gave pure silica except for the presence of tiny calcite specks.

Tridymite, SiO_2, forms orthorhombic vitreous acicular prisms with triple twinning up to three mm long. Tridymite associated with cordierite indicates high temperature crystallization conditions in a SiO_2 saturated environment. *Portlandite*, $Ca(OH)_2$, occurs as small hexagonal scalenohedra associated with calcite crystals and grows on a calcite, Ca-zeolite and Mg-hydrosilicate crust that mantles the voids (Figure 3H). Portlandite is a crucial mineral which is involved in most of the CSH reaction and is commonly found in natural metacarbonate rocks, fumaroles, combustion products and concrete cements. The portlandite–CSH–CASH association is mostly related to the circulation of hyperalkaline fluids in high Ca rocks [41].

5. Discussion of the paragenetic sequence

Colle Fabbri minerals, other reference compositions, and their chemical relationship in terms of SiO_2, CaO and H_2O are illustrated in Figure 5. The para wollastonite + rankinite + gehlenite rock that forms the core of the melilitolite body has an estimated crystallization temperature of 1300°C [3]. The increase in SiO_2 and decrease in Al_2O_3 due to the progressive assimilation of pelite led to the disappearance of rankinite and kalsilite, then melilite and leucite, and the appearance of An. This is possible passing through para wollastonite + gehlenite or para wollastonite + gehlenite + anorthite (1270°C) and via para wollastonite + anorthite to eutectic para wollastonite + anorthite + tridymite (1195°C). Thermometric data show that the wollastonite-anorthite-cpx assemblage in the igneous facies crystallized above a temperature of 1230°C [3]. Clinker fragments produced by heating of the argillite country rocks contain a cordierite-tridymite association, which constrains its initial temperature between 1000 and 1140°C [4]. The red-coloured thermometamorphic argillite probably formed in the 870–1000°C range [3]. It is reasonable to assume that the silicate-carbonate-sulphate association started to crystallize at relatively low temperatures, when fractures could form from the solidified mass and the vesicles and the round amygdales were no longer plastic. Both fractures and vesicles contain concentric layers of concretional fibrous or microcrystalline phases that cannot be texturally regarded as magmatic crystallization product (i.e. *liquidus* phases). Several textural occurrences can be identified. These include isolated vesicles (≪ 1 cm) produced by gas expansion, large amygdalar vugs (1 cm), open fractures (cooling jointing or mechanical) and connected open spaces among breccia clasts. Even if most of these occurrences have only two or three mineral species, it is possible to depict an idealized crystallization sequence or hierarchy based on the concentric layers which infill fractures and larger amygdales.

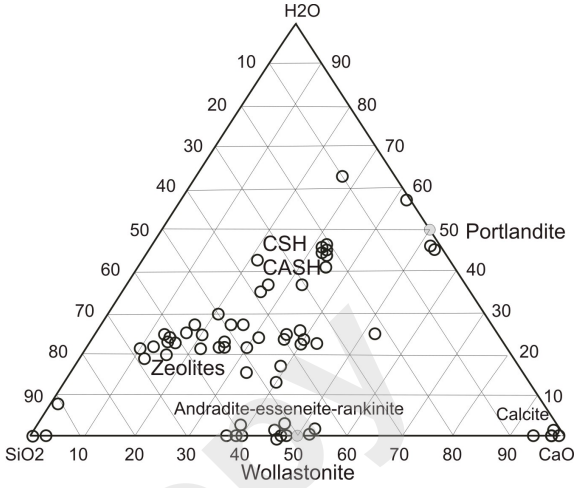

Figure 5. Chemical relationship between CSH-CASH and other mineral phases of CF compared with other relevant mineral compositions in terms of their H_2O-CaO-SiO_2 components.

The selected specimens (CF2 to CF25 above) are representative of the paragenetic sequence, essential to understanding the conditions under which these minerals grow (Tables 1 and 2). Not all mineral phases have been neatly located in the sequence and some are transient compounds passing through one stable stage to another. Based on textural occurrences and distinct mineral associations in each sample, five stages of mineralization may have occurred subsequent to the cooling of this magma. The following sequence is mostly based on petrographic evidences from different paragenetic concentric layers. We assume that pristine layers are relatively older and formed at near igneous conditions. Late layers are assumed to have formed during lowering of the temperature to ambient conditions.

The stages are:

Stage 1 Gas expansion forming small bubbles in the melt that are in contact with argillite clasts infilled by skeletal tridymite+alpha-quartz covered by calcite;

Stage 2 silica and calcite occurring in repeated concentric layers. Layers are made of very fine-grained or colophanic material, followed by microcrystalline tobermorite;

Stage 3 zeolites and strätlingite (radial aggregates up to 1 cm in diameter);

Stage 4 thaumasite, ettringite, jennite, calcite (drusy) and aragonite (microcrystalline);

Stage 5 barite and gypsum.

Stage 1 may be related to high-temperature calcification of argillite in the presence of juvenile gases, indicating a temperature $< 870°C$ but above 600°C as hydromicas are absent. The minerals from Stage 2 to Stage 5 can all be experimentally obtained at room temperature using very fine-grained and reactive compounds, which roughly approximate CF conditions [9, 26]. Only a few experiments have been made, which attempt to describe the natural conditions and reaction dynamics such as melt/rock and hydrothermal-fluid/rock, and these are mostly limited to single zeolites. However, grain size distribution is from colophanic-microcrystalline to coarse-grained and drusy with a central empty vug, and a distinct crystallization sequence accompanied by a chemical variation involving substantial large-ion lithophile elements (i.e. Ba) and OH/H_2O ratios, are features that are likely to be linked to alkaline steam-heated, juvenile and/or connate fluids.
The paragenesis in Stage 2 is simply interpreted as a silica-calcite reaction in the prescence of water/steam. Even though tobermorite can be produced from $Si(OH)_4$ and $CaCl_2$ at temperatures lower than 100°C [42], natural occurrences are mostly related to contact phenomena and a hydrothermal stage $T \approx 350°C$ [43].
Zeolites crystallize together in Stage 3, mostly before cement phases. A reasonable temperature range for this stage of hydrothermal activity would be between ~150 and 200°C.
Stage 4: This kind of deposition was also observed in isolated vesicles and thus has to be regarded as a late cooling stage. This is largely dominated by a sulphate-carbonate-silicate reaction with juvenile-connate water during a post-zeolitic "cement" stage at $T \approx 100°C$.
Stage 5: These are alteration minerals from thaumasite, mostly at near room temperature.

6. Conclusion

Sulphates and hydrated and/or hydroxylated silicate-sulphate-carbonates of CF are rare in silicate igneous rocks, and seem to be restricted to carbonated melts such as carbonatites, kimberlites and kamafugites. The complex nature of the CF mineralization indicates, however, intense metasomatic exchange with argillitic country rocks prompted by locally high temperatures suggested by the occurrence of tridymite and cordierite. This is required because the CF magma is highly SiO_2-Al_2O_3 undersaturated, and such minerals cannot crystallize directly from it.

The effects on country rocks that generate some of these minerals are suggested by the mineral presences in some metacarbonate/pelite rocks, in artificial combustion, and in concrete cements. For example, at Lapanouse de Séverac, Aveyron, Saint-Maime, Alpes-de Haute-Provence, scoria slag is produced by artificial heating of bituminous schists and coal-bearing rocks containing, among other minerals, CSH and zeolites [44, 45]. At CF clear contact between the magmatic body and country rocks allows a distinction to be made between mineral species that have diferenciated chemical compositions based on their igneous or metamorphic origins. It is now clear that, whatever the cause, igneous or pyrometamorphic, hydroxylated silicate-sulphate-carbonates can be generated under transient chemical conditions [46, 47]. Oldhamite is an ephemeral mineral which may form in high-temperature from high-Ca igneous and pyrometamorphic rocks that rapidly hydrate to CSH/CASH in alkaline conditions, with a complex evolutionary process that is typical of Portland cements. At a high Ca melt/argillite interface, CSH and CASH are precipitated instead of zeolite phases. An increase in the Ca/Si ratio in the solid phase converts CSH-CASH into Ca-Ba-zeolites, which then become the predominant crystallizing phases. Willhendersonite and associated Ca-zeolites are usually found in metacarbonate xenoliths in lavas, and have only previously been reported from one other igneous rock, the kalsilite leucite melilitolite of San Venanzo, Italy [33, 48, 49]. It is apparent that CSH-CASH are the dominant products forming by circulation of fluids at the expense of the primary Ca-silicates in the igneous rocks. However, variable precipitation of CSH-CASH, zeolites and other minerals, as well as amorphous phases, is less obvious and different scenarios can be depicted to explain the mineral zoning found at CF. The progressive changes in the mineralogy of concentric layers in amygdales suggest deposition within a cooling system. These fluids were very rich in CO_2, a component which is always very abundant in carbonatite-related magmas [50]. Large-ion lithophile elements such as K, Sr and Ba are distinctively concentrated in the CF minerals such as in kamafugitic melts. A CO_2 aqueous system concentrates and mobilizes hydromagmatophile elements such as K and Ba, which are easily incorporated into a hyperalkaline steam, precipitating complex secondary minerals such as those found at CF. Beside temperature, pressure and chemical conditions, the distribution of the mineralization at CF seems to depend on the differences that occurred in the evolution of the fracturing within the rock, as inferred from field observations and experimental studies [51]. If the reaction + dissolution/precipitation rate is high, the fracture may seal first, thus causing the mineralizing zone to move upstream towards the igneous rock because of limited per-

meability. On the other hand, if the rate is low the igneous rock becomes completely cemented and the hydrothermal plume moves away from the plug toward the contact, producing generation of zones of concentric mineralisation. We think that this is a likely scenario given the observed data.

Further analyses are planned in order to investigate the presence and distribution of the rare earth elements and other high-field-strength elements in the CF secondary minerals. We also need to confirm the presence of thomsonite and possibly rhodesite and levyne. SCXRD studies of the CF outcrop minerals might show more interesting structures and possibly the identification of several new mineralogical species. The latter will form the basis of future research by the authors.

Acknowledgments

We are deeply indebted to and grateful to Philip Neuhoff, Anton Chakhmouradian and Keith Bell for all their suggestions and thoughtful revision of a previous version of the manuscript. We thank Katrazyna Cyran and two anonymous reviewers for their suggestion and editorial assistance.

References

[1] Stoppa F., L'euremite di Colle Fabbri (Spoleto): Un litotipo ad affinità carbonatitica in Italia. Bollettino. Società Geologica Italiana, 1988, 107, 239-248

[2] Stoppa F., Rosatelli G., Ultra-mafic intrusion triggers hydrotermal explosions at Colle Fabbri (Spoleto, Umbria), Italy, J. Volcanol. Geoth. Res., 2009, 187, 85-92

[3] Stoppa F., Sharygin V.V., Melilitolite intrusion and pelite digestion by high temperature kamafugitic magma at Colle Fabbri, Spoleto, Italy, Lithos, 2009, 112, 306-320

[4] Stoppa F., Cundari A., Rosatelli G., Woolley A.R., Leucite melilitolites in Italy: Genetic aspects and relationship with associated alkaline rocks and carbonatites, Periodico di mineralogia, 2003, 72, 223-251

[5] Stoppa F., Rosatelli G., Principe C., Le vulcaniti del Monte Vulture, classificazione modale e considerazioni seriali. In: Principe C. (Ed.) La geologia del Monte Vulture. Regione Basilicata, Dipartimento Ambiente, Territorio e Politiche della Sostenibilità, Lavello 2006, 87-104

[6] Stoppa F., Sharygin V.V., Nyerereite from carbonatite rocks at Vulture volcano:implications for mantle metasomatism andpetrogenesis of alkali carbonate melts. Central European Journal of Geosciences, 2009, 1, 131-151

[7] Ding J., Fu Y., Beaudoin J.J., Strätlingite formation in high-alumina cement-silicate fume systems: Significance of sodium ions. Cement Concrete Res., 1995, 25, 1311-1319

[8] Macphee E. D., Barnett S.J., Solution properties of solids in the ettringite-thaumasite solid solution series., Cement Concrete Res., 2004, 34, 1591-1598

[9] Shimada Y., Young J.F., Thermal stability of ettringite in alkaline solutions at 80°C., Cement Concrete Res., 2004, 2261-2268

[10] Passaglia E., Galli E., Vertumnite, a new natural silicate. Tschermaks Mineralogiche und Petrografische Mitteilungen, 1977, 24, 57-66

[11] Passaglia E., Turioni B., Silicati ed altri minerali di Montalto di Castro (Viterbo), R.M.I. (please expand the acronime), 1982, 4, 97-110

[12] Schüller W., Betz V., Die mineralien vom Emmelberg, Lapis, 1986, 11, 11-25

[13] Taucher J., Von Hollerer C.E., Ein Ca-reicher Xenolith aus dem Basaltsteinbruch Kloch, Nordlicher Bruch, Klocher Klause (Steiermark, Osterreich). Mitt. Naturwiss. Ver. Steiermark, 2000, 130, 19-30

[14] Baumgärtl U., Cruse B., Die Mineralien der Vulkaneifel, Aufschluss, 2007, 58, 257-400

[15] Gross S., The mineralogy of the Hatrurim Formation, Israel, Geol. Surv. Isr. Bull., 1977, 70, 1-80

[16] Sharygin V.V., Sokol E.V., Vapnik Y., Minerals of the pseudobinary perovskite-brownmillerite series from combustion metamorphic larnite rocks of the Hatrurim Formation, Israel, Russ. Geol. Geophys., 2008, 49, 709-726

[17] Barker D.S., Nixon P.H., High–Ca, low alkali carbonatite volcanism at Fort Portal, Uganda, Contrib. Mineral. and Petr., 1989, 130, 166-177

[18] Wheeler S., Spigarelli S., Stoppa F., Rinaldi R., Secondary minerals from the igneous complex of Colle Fabbri, Spoleto (PG), Plinius, 1996, 16, 211-212

[19] Hentschel G., Die Lavaströme der Graulai: eine neue Fundstelle in der Westeifel, Lapis, 1993, 18, 11-23

[20] Bruker, SAINT v7.60A. Bruker AXS Inc., Madison, Wisconsin, USA, 2009

[21] Sheldrik G. M., SADABS, University of Göttigen, Germany, 2002

[22] Sheldrik G. M., XPREP, University of Göttigen, Germany, 2007.

[23] Bonaccorsi E., Merlino S., Calcium silicate hydrate (CSH) minerals: Structures and transformations, 32nd International Geological Congress, Florence, Italy, 20-28 August 2004, Abstract Volume, 2004, 215

[24] Bonaccorsi E., Merlino S., Kamph A. The crystal structure of tobermorite 14 Å (plombierite), a C-S-H phase, J. Am. Ceram. Soc., 2005, 88, 505-512
[25] Parry J., Wright F.E., Afwillite, a new hydrous calcium silicate, from Dutoitspan Mine, Kimberley, South Africa. Mineral. Mag., 1925, 20, 277-285
[26] Zhou Q., Lachowski E.E., Glasser F.P., Metaettringite, a decomposition product of ettringite. Cement Concrete Res., 2004, 34, 703-710
[27] Edge R.A., Taylor H.F.W., Crystal Structure of Thaumasite, $[Ca_3Si(OH)_6\ 12H_2O](SO_4)(CO_3)$, Acta Cryst., 1971, B27, 594
[28] Rinaldi R., Sacerdoti M., Passaglia E., Strätlinigite: crystal structure, chemistry and a re-examination of its polytype vertumnite, Eur. J. Mineral., 1990, 2, 841-849
[29] Galli E., Passaglia E., Vertumnite: Its crystal structure and relationship with natural and synthetic phases, Tschermacks Min. Petr. Mitt., 1978, 25, 33-46
[30] Coombs D.S., Alberti A., Armbrutser T., Artioli G., Galli E., Grice J.D., Liebau F., Minato H., et al., G. Recommended nomenclature for zeolite minerals: Report of the subcommittee on zeolites of the international mineralogical association, commission on new minerals and mineral names. The Canadian Mineralogist, 1997, 35, 1571-1606
[31] Mazzi F., Galli E., The tetrahedral framework of chabazite. Neues Jahrb. Mineral., Monatsh., 1983, 461-480
[32] Gottardi G., Galli E., Natural Zeolites, Springer-Verlag, Berlin, 1985
[33] Stoppa F., Sharygin V.V., Cundari A., New mineral data from the kamafugite-carbonatite association: The melilitolite from Pian di Celle, Italy. Miner. Petrol., 1997, 61, 27-45
[34] Postl W., Walter F., Tetranatrolith aus dem Basaltbruch Stürgkh-Hrusak in Klöch, Steiermark. In: Niedermayr G, Postl W, Walter F., Eds., Neue Mineralfunde aus Österreich XXXIV, Carinthia II, 1985, 175, 250
[35] Blass G., Graf H.W., Neufunde von bekannten Fundorten (VIII), Mineralien-Welt, 1993, 5, 41-48
[36] Rinaldi R., Pluth J.J., Smith J.V., Zeolites of the phillipsite family. Refinement of the crystal structures of phillipsite and harmotome, Acta Crystallogr., 1974, D.30, 2426–2433
[37] Gualtieri A.F., Accurancy of XRPD OPA using the combined Ritveld-RIR method. J. Appl. Crystallogr., 2000, 33, 267-278
[38] Gatta G.D., Cappelletti P., Rotiroti N., Slebodnick C., Rinaldi R., New insights into the crystal structure and crystal chemetry of the zeolite phillipsite. Am. Mineral., 2009, 94, 190-199
[39] Passaglia E., Pongiluppi D., Rinaldi R., Merlinoite, A new mineral of the zeolite group. Neues Jahrb. Mineal., Monatsh., 1977, 355-364
[40] Moore A.E., Taylor H.F.W., Crystal Structure of Ettringite, Acta Cryst., 1970, B26, 386
[41] Steefela C.I, Lichtnerb P.C., Multicomponent reactive transport in discrete fractures II: Infiltration of hyperalkaline groundwater at Maqarin, Jordan, a natural analogue site, J. Hydrol., 1998, 209, 200-224
[42] Suzuki S., Sinn E., 1.4 nm tobermorite-like calcium silicate hydrate prepared at room temperature from $Si(OH)_4$ and $CaCl_2$ solutions, J. Mater. Sci.Lett., 1992, 12, 542-544
[43] Diamond S., White J.L., Dolch W.L., Effects of isomorphous substitution in hydrothermally-synthesized tobermorite, Am. Mineral., 1966, 51, 388-401
[44] Eytier C., Eytier J.R., Favreau G., Devouard B., Vigier J., Minéraux de pyrométamorphisme de Lapanouse de Severac (Aveuron), Cahier des Micromonteurs, 2004, 85, 3-32
[45] Favreau G., Meisser N., Chiappero P.J., Saint-Maime (alpes-de-Haute-Provence): Un Exemple de pyrométamorphisme en région provençale, Cahier des Micromonteurs, 2004, 85, 59-91
[46] Capitanio F., Comment on Melluso et al. (2003). The Ricetto and Colle Fabbri wollastonite and melilite-bearing rocks of the central Apennines, Italy, Am. Mineral., 2005, 90, 1934-1939
[47] Stoppa F, Rosatelli G., Cundari A., Castorina F., Woolley, A.R., Comments on Melluso et al. (2003) and their reported data and interpretation of some wollastonite- and melilite-bearing rocks from the Central Apennines of Italy, Am. Mineral., 2005, 90, 1919-1925
[48] Peacor D.R., Dunn P.J., Simmons W.B., Tillmanns E., Fisher R.X., Willhendersonite, a new zeolite isostructural with chabazite, Am. Mineralogist, 1984, 69, 186-189
[49] Tillmanns E., Fischer R.X., Baur W.H., Chabazite-type framework in the new zeolite willhendersonite. Neues Jahrb, Mineral. Monatsh., 1984, 547-558
[50] Stoppa F., Lloyd F.E., Rosatelli G., CO_2 as the propellant of carbonatite–kamafugite cognate pairs and the eruption of diatremic tuffisite. Periodico di Mineralogia, Special Issue, Eurocarb, 2003, 72, 205-222
[51] Steefela C.I, Lichtnerb P.C., Multicomponent reactive transport in discrete fractures II: Infiltration of hyperalkaline groundwater at Maqarin, Jordan, a natural analogue site. J. Hydrol., 1998, 209, 200-224